

## A CURVE EVOLUTION-BASED VARIATIONAL APPROACH TO SIMULTANEOUS IMAGE RESTORATION AND SEGMENTATION

Junmo Kim, Andy Tsai, Mujdat Cetin, and Alan S. Willsky

Laboratory for Information and Decision Systems, Massachusetts Institute of Technology  
77 Massachusetts Ave., Cambridge, MA 02139, USA

### ABSTRACT

In this paper, we introduce a novel approach for simultaneous restoration and segmentation of blurred, noisy images by approaching a variant of the Mumford-Shah functional from a curve evolution perspective. In particular, by viewing the active contour as the set of discontinuities in the image, we derive a gradient flow to minimize an extended Mumford-Shah functional where the known blurring function is incorporated as part of the data fidelity term. Each gradient step involves solving a discrete approximation of the corresponding partial differential equation to obtain a smooth and deblurred estimate of the observed image without blurring across the curve. The experimental results based on both synthetic and real images demonstrate that the proposed method segments and restores the blurred images effectively. We conclude that our work is an edge-preserving image restoration technique that couples segmentation, denoising, and deblurring within a single framework. In addition, this framework provides an intellectual connection between regularization theory (used to solve the deblurring inverse problem) and the theory of curve evolution.

### 1. INTRODUCTION

An important inverse problem in image processing is the problem of estimating underlying scenes from blurred and noisy observed images. In general, this is an ill-posed problem, and techniques based on regularization theory have been favored for its solution. The most common regularization approach is Tikhonov regularization [14]. Such methods lead to computationally straightforward optimization problems, but they may suppress useful features in the resulting imagery, such as edges. Recently, considerable efforts have been spent in designing alternative techniques which preserve boundaries between regions, while performing the regularization [16, 5]. Our interest is in obtaining such a robust regularization of the inverse problem, but at the same time explicitly segmenting the image. To this end, we propose an algorithmic framework for image deblurring and *segmentation*.

One approach to image segmentation is via curve evolution techniques [1, 2, 3, 6, 11, 12, 17, 18]. In general, the goal of these techniques is to extract the boundaries (represented by closed curves) within an image. Recently, a new curve evolution approach based on minimizing the original Mumford-Shah functional [7, 8] has been proposed for simultaneous smoothing and segmentation of noisy images [4, 15]. The image smoothing proposed in this work is linear, with edge preservations based on a global segmentation of the

image by the curve. In this paper, we demonstrate how we extend the technique in [15] to an edge-preserving deblurring and denoising algorithm. The major novelty of our approach is the solution of the image restoration problem in a curve evolution framework, which leads to an explicit segmentation of the image as well as a solution of the restoration problem.

The remainder of the paper is organized as follows. Section 2 formulates our approach to solving the inverse problem from a curve evolution perspective. In particular, an objective functional is constructed based on an extended form of the Mumford-Shah functional. Section 3 then derives our curve evolution-based approach to minimizing this objective functional. We present experimental results in Section 4, using both synthetic and real images. Finally, we conclude in Section 5 with a summary and some further research directions.

### 2. THE EXTENDED MUMFORD-SHAH FUNCTIONAL FOR THE RESTORATION PROBLEM

A variant of the Mumford-Shah functional where discontinuities are limited to a closed curve is given by

$$E_0(f, \vec{C}) = \beta \iint_{\Omega} (f - g)^2 dA + \alpha \iint_{\Omega \setminus \vec{C}} |\nabla f|^2 dA + \gamma \oint_{\vec{C}} ds \quad (1)$$

in which  $\vec{C}$  denotes the smooth, closed segmenting curve,  $g$  denotes the observed data,  $f$  denotes the piecewise smooth approximation to  $g$  with discontinuities only along  $\vec{C}$ , and  $\Omega$  denotes the image domain [8, 7]. Note that the first term in  $E_0(f, \vec{C})$ , the data fidelity term, is proportional to the negative-log-likelihood of observing  $g$  given  $f$ , for the observation model

$$g(x, y) = f(x, y) + n(x, y), \quad (2)$$

where  $(x, y)$  denotes the coordinates in  $\mathbf{R}^2$ , and  $n$  is white Gaussian noise. With a statistical maximum a posteriori (MAP) estimation perspective, the second and the third terms in (1) are related to the prior probability density functions on  $f$  and  $\vec{C}$ .

The observation model for the deblurring problem we are interested in solving is

$$g(x, y) = h(x, y) * f(x, y) + n(x, y), \quad (3)$$

where  $h$  is a *known* 2-D impulse response of the blurring operation. For this observation model, we can formulate an extended

---

This work was supported by the Office of Naval Research under Grant N00014-00-1-0089, and the Air Force Office of Scientific Research under Grant F49620-00-0362.

Mumford-Shah functional based on the same prior assumptions as in (1) about  $f$  and  $\vec{C}$ :

$$E(f, \vec{C}) = \beta \iint_{\Omega} (h * f - g)^2 dA + \alpha \iint_{\Omega \setminus \vec{C}} |\nabla f|^2 dA + \gamma \oint_{\vec{C}} ds \quad (4)$$

This is the objective function we will minimize.

### 3. MINIMIZATION OF THE EXTENDED MUMFORD-SHAH FUNCTIONAL

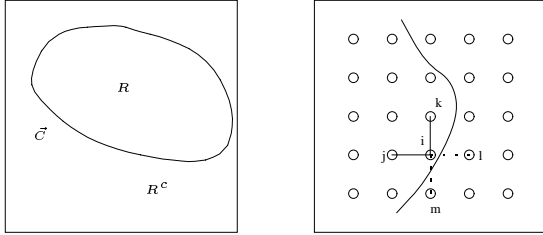


**Fig. 1.** Illustration of the curve ( $\vec{C}$ ), the region inside the curve ( $R$ ), the region outside the curve ( $R^c$ ), and the discrete lattice overlaid with the curve.

In this section, we present a discrete implementation to minimize the extended Mumford-Shah functional of (4). First, the discrete version of the observation model (3) is given by

$$\mathbf{g} = \mathbf{H}\mathbf{f} + \mathbf{n}, \quad (5)$$

where  $\mathbf{f}$  and  $\mathbf{g}$  are real-valued vectors consisting of a lexicographic ordering of pixels in the underlying and the observed images respectively,  $\mathbf{H}$  is the blurring matrix, and  $\mathbf{n}$  is white Gaussian noise. The corresponding discrete version of the extended Mumford-Shah functional is

$$E(\mathbf{f}, \vec{C}) = \beta \|\mathbf{H}\mathbf{f} - \mathbf{g}\|^2 + \alpha \sum_{(i,j) \in S} (f_i - f_j)^2 + \gamma \oint_{\vec{C}} ds \quad (6)$$

where  $S = \{(i, j) | i, j \text{ are adjacent in the lattice, and } i, j \text{ are in the same side of the curve } \vec{C}\}$ , and  $f_i$  and  $g_i$  denote the  $i$ th components of  $\mathbf{f}$  and  $\mathbf{g}$  respectively. Figure 1 illustrates that  $(i, j)$  and  $(i, k)$  are in  $S$ , whereas  $(i, l)$  and  $(i, m)$  are not in  $S$ .

Now the problem is to find  $\mathbf{f}$  and  $\vec{C}$  that minimize  $E(\mathbf{f}, \vec{C})$  of (6). We propose an iterative optimization scheme where each iteration consists of two steps. The first step calculates  $\mathbf{f}$  that minimizes  $E(\mathbf{f}, \vec{C})$  given  $\vec{C}$ . The necessary condition for such an  $\mathbf{f}$  is given by a linear equation (a discrete approximation of a partial differential equation (PDE)). The second step evolves the curve by  $\vec{C}_t$ , which is the negative of the gradient of  $E(\mathbf{f}(\vec{C}), \vec{C})$ . The algorithm is summarized by the following pseudo code:

```
initialize  $\vec{C}$ ;
while (not converged) {
```

```
    solve  $\mathbf{f} = \arg \min_{\mathbf{f}} E(\mathbf{f}, \vec{C})$  for fixed  $\vec{C}$ ; (Section 3.1)
    evolve the curve with  $\vec{C}_t$ ; (Section 3.2)
```

} where the convergence criterion is

$$\frac{\|\mathbf{f}_{\text{prev.}} - \mathbf{f}_{\text{new}}\|}{\|\mathbf{f}_{\text{prev.}}\|} < \epsilon, \text{ where } \epsilon \text{ is a small positive constant.}$$

#### 3.1. Estimation of the Field by a Linear Equation

We can find a necessary condition on  $\mathbf{f}$  by calculating the first derivative of  $E$  with respect to  $f_i$  for each  $i$ . Let  $\mathbf{h}_i$  be the  $i$ th column of the matrix  $\mathbf{H}$ , so that  $\mathbf{H}\mathbf{f} = \sum_i \mathbf{h}_i f_i$ . Then the first derivative of  $E$  with respect to  $f_i$  is given by

$$\frac{\partial E}{\partial f_i} = 2\beta \sum_j \mathbf{h}_i^T \mathbf{h}_j f_j - 2\beta \mathbf{h}_i^T \mathbf{g} + 2\alpha \sum_{j \text{ s.t. } (i,j) \in S} (f_i - f_j) \quad (7)$$

Then the necessary condition  $\frac{\partial E}{\partial f_i} = 0$  for each  $i$  is

$$\sum_j \mathbf{h}_i^T \mathbf{h}_j f_j - \frac{\alpha}{\beta} \sum_{j \text{ s.t. } (i,j) \in S} (f_j - f_i) = \mathbf{h}_i^T \mathbf{g}. \quad (8)$$

Finally, the necessary condition on  $\mathbf{f}$  is given by the following linear equation, whose  $i$ th row is (8):

$$\mathbf{H}^T \mathbf{H}\mathbf{f} - \frac{\alpha}{\beta} \mathbf{A}\mathbf{f} = \mathbf{H}^T \mathbf{g}, \quad (9)$$

where

$$\mathbf{A}_{ij} = \begin{cases} 1 & \text{if } (i, j) \in S \\ -\sum_{k \text{ s.t. } (i,k) \in S} \mathbf{A}_{ik} & \text{if } i = j \\ 0 & \text{otherwise} \end{cases}. \quad (10)$$

Note that the matrix  $\mathbf{A}$ , which depends on the current position of the curve, is a discrete implementation of the operator  $\nabla^2$  which does not take differences across the curve. Thus this linear equation is a discrete approximation of a PDE. In our work, the above linear equation is solved by the conjugate gradient method.

#### 3.2. Curve Evolution

Now we need to look at the variation of  $E$  with respect to the curve  $\vec{C}$ . First, since only the data fidelity term in our extended objective functional is different from the original Mumford-Shah functional, the variation with respect to the curve is very similar to that derived in [7]. A rigorous derivation of the variation is beyond the scope of this paper, so we refer the reader to [7] for further details, and here we give an intuitive explanation. The idea is to move the curve around a point of index  $i$  (whose intensity is  $f_i$ ) adjacent to the curve. At such a point adjacent to the boundary, there is a competition between  $R$  (the region inside the curve) and  $R^c$  (the region outside the curve). In other words, the competition is to decide whether to put the point  $i$  in  $R$  or in  $R^c$ .

Note that moving the curve such that the point  $i$  becomes inside the curve changes the image intensity of that point by an extension of  $f$  from  $R$ , while keeping the image intensity of the other points unchanged [7]. Similarly, moving the curve such that the point  $i$  becomes outside the curve replaces the image intensity of that point

by an extension of  $f$  from  $R^c$ . Thus the contribution from the data fidelity term to the gradient of the energy with respect to the curve is given by the difference between the two evaluations of this data fidelity term for the two possible choices of  $f_i$ . Thus the curve evolution is given by

$$\vec{C}_t = \beta D \vec{N} + \alpha P \vec{N} - \gamma \kappa \vec{N}, \quad (11)$$

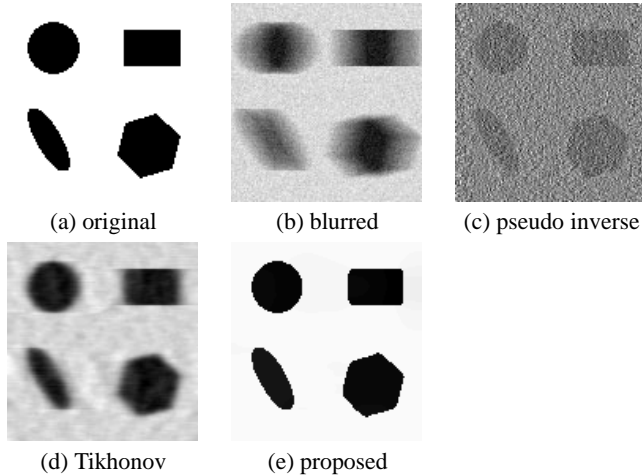
where

$$\begin{aligned} D &= \|\mathbf{H}\mathbf{f} - \mathbf{g}\|_{f_i=f_{R^c}}^2 - \|\mathbf{H}\mathbf{f} - \mathbf{g}\|_{f_i=f_R}^2 \\ P &= \sum_{\substack{j \in R^c \\ j \text{ is adjacent to } i}} (f_i - f_j)^2 \\ &\quad - \sum_{\substack{j \in R \\ j \text{ is adjacent to } i}} (f_i - f_j)^2, \end{aligned}$$

$\kappa$  is the curvature, and  $\vec{N}$  is the outward normal vector of the curve  $\vec{C}$ . The curve evolution is implemented by using standard level set methods [13, 9, 10].

#### 4. EXPERIMENTAL RESULTS

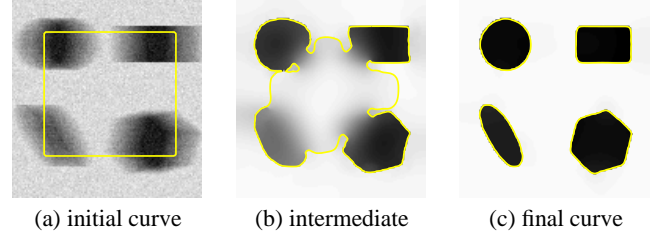
We present experimental results on a synthetic image of  $126 \times 121$  pixels and a real image of an aircraft of  $480 \times 270$  pixels. We consider a problem involving the restoration and segmentation of images distorted by a spatially invariant horizontal motion blur. The distorted data are obtained by applying a 25-pixel horizontal motion blur to the original image followed by the addition of white Gaussian noise, where the resulting signal to noise ratio (SNR)<sup>1</sup> is 16.1 dB for the synthetic image and 13.2 dB for the aircraft image.



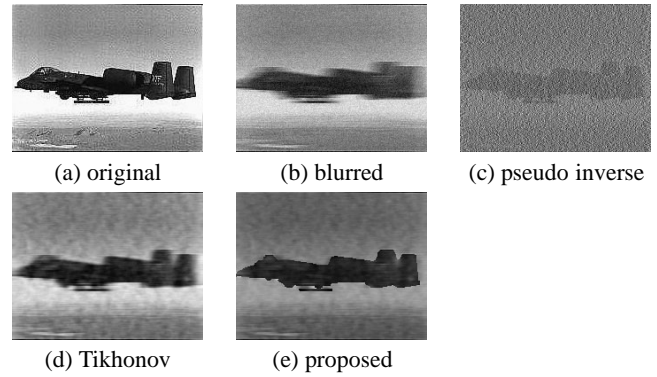
**Fig. 2.** Comparison of the restoration results on a synthetic image.

Figure 2 illustrates the restoration results on the synthetic image. The original image is shown in Figure 2(a), and the blurred

<sup>1</sup>SNR  $\triangleq 10 \log_{10} \left( \frac{\text{Var}(\mathbf{H}\mathbf{f})}{\text{Var}(\mathbf{n})} \right)$ , where  $\text{Var}(Z)$  denotes the variance of  $Z$ .



**Fig. 3.** Evolution of the curve and the final segmentation result on a synthetic image.



**Fig. 4.** Comparison of the restoration results on an aircraft image.

and noisy observed image is shown in Figure 2(b). To demonstrate the ill-conditioned nature of the problem, we show the restoration obtained by running the observed data through the pseudo inverse of the blurring kernel in Figure 2(c). As it is well-known, such an inversion exhibits severe noise amplification, which we observe in Figure 2(c). Figure 2(d) shows the image restoration result of Tikhonov regularization. Note that some deblurring is achieved, and some smoothness is imposed. However, the sharp boundaries between the regions are not successfully restored. Finally, the result of our proposed method based on the Mumford-Shah functional is shown in Figure 2(e). This result is visually much closer to the original image of Figure 2(a) than the Tikhonov solution shown in Figure 2(d).

Note that restoration results similar to Figure 2(e) can also be obtained by other edge-preserving regularization methods. However, as described in Section 3, our method also provides an explicit segmentation through its curve evolution-based structure, which we

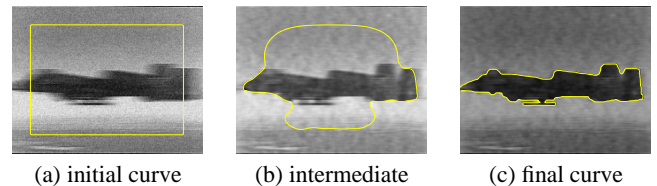


**Fig. 5.** Evolution of the curve and the final segmentation result on an aircraft image.

illustrate in Figure 3. Figure 3(a) shows the initial curve  $\vec{C}$  on the observed image. In Figure 3(b), we display the curve at an intermediate iteration, together with the corresponding estimated field. Finally, Figure 3(c) shows the final curve and the corresponding segmented image at convergence. This result shows that our method can detect the boundaries of the objects and restore the image effectively.

We now report the results of similar experiments for a real aircraft image. The original scene, the observed image, and the restored image based on the pseudo inverse are shown in Figure 4(a), 4(b), and 4(c) respectively. Figure 4(d) contains the Tikhonov solution, whereas Figure 4(e) displays the result of our technique. Our method appears to produce a good piecewise smooth approximation of the original image. Again, using boundary information enables deblurring and denoising without losing sharpness of the edges. In Figure 5, we demonstrate samples from the evolution of the curve and the resulting segmentation, which seems to capture the boundaries of the aircraft successfully.

## 5. CONCLUSIONS

We have presented a novel technique for robust restoration and segmentation of images by combining and extending ideas from variational methods for edge-preserving regularization and the theory of curve evolution. In particular, we have derived a curve evolution formula to minimize a variant of the Mumford-Shah functional, which incorporates a model of the observation process and an explicit representation of the region boundaries through an active contour.

We have presented results demonstrating the effectiveness of our method in restoring and segmenting synthetic and real images. Our current work involves extensions and applications of our technique to other inverse problems such as computed tomography.

## 6. REFERENCES

- [1] V. Caselles, F. Catte, T. Coll, and F. Dibos, "A geometric model for active contours in image processing," *Numerische Mathematik*, vol. 66, pp. 1–31, 1993.
- [2] V. Caselles, R. Kimmel, and G. Sapiro, "Geodesic snakes," *Int. J. Computer Vision*, 1998.
- [3] T. F. Chan and L. A. Vese, "Active contours without edges," *IEEE Trans. on Image Processing*, vol. 10, no. 2, pp. 266–277, Feb. 2001.
- [4] T. Chan and L. Vese, "A level set algorithm for minimizing the Mumford-Shah functional in image processing," *UCLA Technical Report*, 2000.
- [5] P. Charbonnier, L. Blanc-Féraud, G. Aubert, and M. Barlaud, "Deterministic edge-preserving regularization in computed imaging," *IEEE Trans. on Image Processing*, vol. 6, no. 2, pp. 298–310, February 1997.
- [6] R. Malladi, J. Sethian, and B. Vemuri, "Shape modeling with front propagation: a level set approach," *IEEE Trans. Pattern Anal. Machine Intell.*, vol. 17, pp. 158–175, 1995.
- [7] D. Mumford and J. Shah, "Optimal approximations by piecewise smooth functions and associated variational problems," *Communications in Pure and Applied Mathematics*, vol. 42, no. 4, 1989.
- [8] D. Mumford and J. Shah, "Boundary detection by minimizing functionals," *Proc. IEEE Conf. Computer Vision and Pattern Recognition*, 1985.
- [9] S. Osher, "Riemann solvers, the entropy condition, and difference approximations," *SIAM J. Numer. Anal.*, vol. 21, pp. 217–235, 1984.
- [10] S. Osher and J. Sethian, "Fronts propagation with curvature dependent speed: Algorithms based on Hamilton-Jacobi formulations," *Journal of Computational Physics*, vol. 79, pp. 12–49, 1988.
- [11] N. Paragios and R. Deriche, "Geodesic active regions and Level Set Methods for Supervised Texture Segmentation," *Int. J. Computer Vision*, 2002.
- [12] R. Ronfard, "Region-based strategies for active contour models," *Int. J. Computer Vision*, vol. 13, pp. 229–251, 1994.
- [13] J. A. Sethian, *Level Set Methods: Evolving Interfaces in Geometry, Fluid Mechanics, Computer Vision, and Materials Science*, Cambridge University Press, 1996.
- [14] A. N. Tikhonov, "Regularization of incorrectly posed problems," *Soviet Math. Dokl.*, vol. 4, pp. 1624–1627, 1963.
- [15] A. Tsai, A. Yezzi, and A. Willsky, "A curve evolution approach to smoothing and segmentation using the Mumford-Shah functional," *Proc. IEEE Conf. Computer Vision and Pattern Recognition*, June 2000.
- [16] C. R. Vogel and M. E. Oman, "Fast, robust total variation-based reconstruction of noisy, blurred images," *IEEE Trans. on Image Processing*, vol. 7, no. 6, pp. 813–824, June 1998.
- [17] A. Yezzi, S. Kichenassamy, A. Kumar, P. Olver, and A. Tannenbaum, "A geometric snake model for segmentation of medical imagery," *IEEE Trans. Medical Imaging*, vol. 16, pp. 199–209, 1997.
- [18] A. Yezzi, A. Tsai, and A. Willsky, "A statistical approach to snakes for bimodal and trimodal imagery," *Int. Conf. on Computer Vision*, 1999.